

Structural signatures of mobility on intermediate time scales in a supercooled fluid

William P. Krekelberg,¹ Venkat Ganesan,¹ and Thomas M. Truskett^{1,2,*}

¹*Department of Chemical Engineering, University of Texas at Austin, Austin, TX 78712.*

²*Institute for Theoretical Chemistry, University of Texas at Austin, Austin, TX 78712.*

We use computer simulations to explore the manner in which the particle displacements on intermediate time scales in supercooled fluids correlate to their dynamic structural environment. The fluid we study, a binary mixture of hard spheres, exhibits classic signatures of dynamic heterogeneity, including a bifurcated single-particle displacement distribution (i.e., subpopulations of immobile and mobile particles). We find that immobile particles, during the course of their displacements, exhibit stronger average pair correlations to their neighbors than mobile particles, but not necessarily higher average coordination numbers. We discuss how the correlation between structure and single-particle dynamics depends on observation time.

When fluids are supercooled (or overcompressed) toward their glass transition, their single-particle dynamics undergo qualitative changes.^{1–7} One example is the emergence of dynamic heterogeneity at time scales intermediate between ballistic and diffusive regimes of particle motion, which manifests as spatially dependent relaxation processes in the liquid^{2,6,8–17} and bifurcated (multi-peaked) probability distributions associated with single-particle displacements. The latter suggests the presence of distinct subpopulations of particles with different mobilities on these time scales.^{7,18–22} Dynamic heterogeneities of this sort continue to attract wide interest because of their perceived consequences for other processes in deeply supercooled liquids including the breakdown of the Stokes-Einstein relationship^{6,18,23–25} and the emergence of non-exponential trends in relaxation of the structure factor.^{6,26}

Several recent studies have systematically explored the extent to which a fluid’s particle configuration at a given time influences the spatial distribution of relaxation processes that immediately follow.^{27–32} Other investigations have focused on probing how certain static structural properties of fluids can be used to correlate the effects that temperature, density, external fields, and interparticle potential have on long-time dynamics.^{33–38} Here, we explore a different, but related, question. Does the local structure surrounding particles in a deeply supercooled liquid, averaged over an intermediate time scale relevant for dynamic heterogeneities, strongly correlate with their mean-square displacements during the period of observation? In other words, do particles with high mobility sample more disordered structural environments during the course of their displacements than those with low mobility and vice versa?

We investigate this question via event-driven⁴¹ molecular dynamics simulation of dense binary fluid mixtures of hard spheres. We set the ratio of particle diameters in these mixtures to $\sigma_1/\sigma_2 = 1.3$ and the ratio of particle masses to $m_1/m_2 = (\sigma_1/\sigma_2)^3$, parameters that mimic concentrated colloidal suspensions that were recently investigated experimentally.⁴² We simulate $N_1 = N_2 = 1000$ particles in a periodically-replicated cubic cell of volume V . We present results for parti-

cle packing fractions $\varphi = \pi(N_1\sigma_1^3 + N_2\sigma_2^3)/6V$ of 0.57 and 0.582, which, as we show below, correspond to state points with unimodal and bifurcated displacement distributions on intermediate time scales, respectively. For brevity, we report quantities that are implicitly nondimensionalized by appropriate combinations of the length scale, $l_c = \sigma_2$ and time scale $t_c = \sqrt{m_2\sigma_2^2/k_B T}$, where k_B is Boltzmann’s constant. We focus on the dynamics and structure of the smaller type 2 particles, but we note that the behavior of the larger type 1 particles (not shown here) is qualitatively similar, as might be expected given the mild particle-size asymmetry of the fluid.

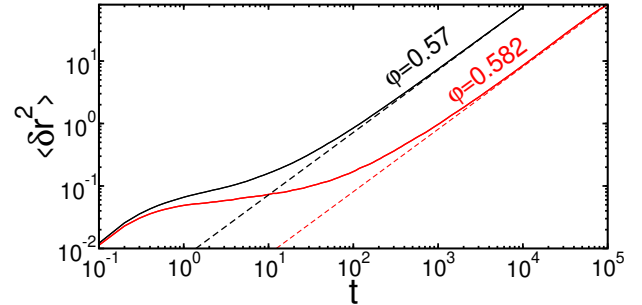


FIG. 1: (Color online) Mean-square displacement $\langle \delta r^2 \rangle$ of the smaller (type 2) particles versus time t at packing fraction $\varphi = 0.57$ (black) and 0.582 (red). Dashed lines are fits of the Einstein relation $\langle \delta r^2 \rangle = 6Dt$ to the long-time behavior, resulting in tracer diffusion coefficients of $D = 1.2 \times 10^{-3}$ and 1.5×10^{-4} at $\varphi = 0.57$ and 0.582, respectively.

We begin by examining the time t dependence of the average mean-square displacement, $\langle \delta r^2 \rangle$, for the type 2 particles. In particular, Figure 1 displays results for packing fractions of $\varphi = 0.57$ and 0.582. At both state points, the fluid exhibits a mean-square displacement plateau at intermediate times, which is characteristic of “cage” dynamics.⁴³ Schematically, the plateau separates the ballistic motion that occurs at very short times (before motion is temporarily hindered by collisions with the cage of nearest-neighbor particles) and the diffusive motion that particles ultimately exhibit at long times (after breaking through the cage). As should be expected, the plateau occurs at smaller displacements and persists

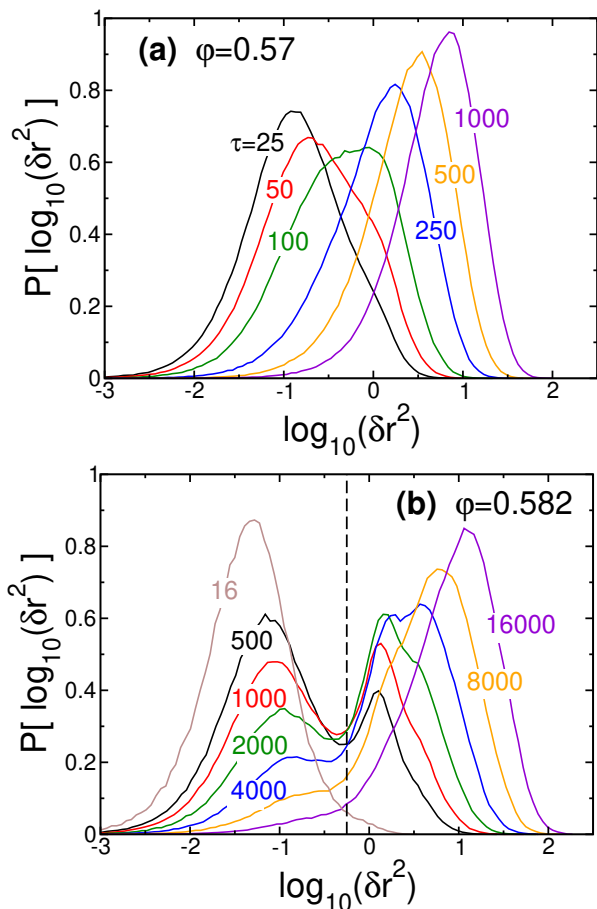


FIG. 2: (Color online) Distribution of the logarithm of mean-square displacement $P[\log_{10}(\delta r^2)]$ for type 2 particles of the binary hard-sphere mixture described in the text. Data cover several time intervals $t = \tau$ for packing fractions **(a)** $\varphi = 0.57$ and **(b)** $\varphi = 0.582$. The numbers in the figure provide the value of τ for each curve. In **(b)**, the vertical line is at $\delta r^2 = 0.56$, the approximate dividing line between mobile and immobile particles discussed in the text.

for longer times when φ is increased, indicating that the cage formed by the nearest-neighbor coordination shell becomes both tighter and more difficult to disrupt at higher packing fraction.

In order to characterize dynamic heterogeneities of the type 2 particles at the state points examined above, we follow Ref. 44 and investigate the distributions of the logarithm of the mean-square displacement ($P[\log_{10}(\delta r^2)]$) over a variety of time intervals ($t = \tau$). Specifically, Figure 2a displays $P[\log_{10}(\delta r^2)]$ for the fluid at $\varphi = 0.57$ and values of τ that correspond to average mean-square displacements which span from the plateau “cage” region to the beginning of the diffusive regime (see Figure 1). The main point of Figure 2a is that, for all values of τ , $P[\log_{10}(\delta r^2)]$ remains unimodal, indicating that pronounced single-particle dynamic heterogeneities have not yet emerged in the fluid at this packing fraction. However, also notice that for the displacement distribu-

tions corresponding to intermediate times, particularly at $\tau = 50$, a shoulder at higher mean-square displacements becomes evident. This shoulder is a precursor to the bifurcated displacement behavior that occurs at $\varphi = 0.582$, which we discuss in detail below.

Figure 2b displays the behavior of $P[\log_{10}(\delta r^2)]$ at $\varphi = 0.582$. Notice that, for intermediate times before diffusive behavior is reached ($500 \leq \tau \leq 4000$), $P[\log_{10}(\delta r^2)]$ shows signatures of bimodality, i.e., two-peak structure. This suggests that subpopulations of mobile and immobile particles are emerging. A qualitative dividing line between the two subpopulations can be drawn at $\delta r^2 \approx 0.56$ (vertical dashed line in Figure 1), which distinguishes the particles that are still caged (i.e., localized) on intermediate time scales from those that have broken through their nearest-neighbor coordination shells to attain larger displacements. For descriptive purposes, we label particles with $\delta r^2 < 0.56$ “immobile” (on these time scales), while we label those with $\delta r^2 > 0.56$ “mobile”. The type of dynamic behavior depicted in Figure 2b has been well documented in other systems.⁴⁵ Below we investigate whether the immobile particles experience, on average, a more ordered structural environment than the mobile particles during the time intervals of their respective displacements.

To carry out the analysis described above, we first examine our simulation trajectories to accumulate statistics for each time interval τ , classifying type 2 particles according to the logarithm of their mean-square displacement during the observation period. This amounts to creating a histogram from the distributions shown in Figures 2a and 2b, assigning type 2 particles to “mobility bins”. Depending on the value of τ , we use bin sizes for $\log_{10}(\delta r^2)$ in the range 0.1 - 0.2, which we find is sufficiently narrow to capture the shapes of the mobility distributions, but coarse enough to allow for excellent statistical sampling. Following Ref. 46, we compute an average pair correlation function, $\tilde{g}_{2j}(r)$, between the type 2 particles in a particular τ -dependent mobility bin and *all* surrounding particles of type j . In determining $\tilde{g}_{2j}(r)$, the relevant pair separations are computed from configurations sampled uniformly in time throughout the time interval of length τ . In this work, we use the \sim overbar to denote a quantity that describes an average dynamic structure surrounding the type 2 particles belonging to a specific mobility bin for a given time interval τ .

In order to convert the τ -dependent structural information contained in the $\tilde{g}_{2j}(r)$ into a number that characterizes the degree of average pair translational order that a type 2 particle (in given a mobility bin) experiences during the course of its displacement, we compute $-\tilde{s}_2$, which we define as

$$-\tilde{s}_2 \equiv \frac{\rho}{2} \sum_j x_j \int_0^\infty d\mathbf{r} \{ \tilde{g}_{2j}(\mathbf{r}) \ln \tilde{g}_{2j}(\mathbf{r}) - [\tilde{g}_{2j}(\mathbf{r}) - 1] \}. \quad (1)$$

Here, $\rho = (N_1 + N_2)/V$ is the total number density, and x_j is the mole fraction of component j . This measure

is a dynamic generalization of a static structural metric, $-s_2^{(2)}$, which quantifies the contribution to the excess entropy of a mixture arising from equilibrium pair correlations involving particles of type 2. Our motivation for using $-\tilde{s}_2$ in this study comes from (1) the earlier empirical observation^{47,48} that the long-time tracer diffusivity of species i in equilibrium mixtures scales in a simple way with the static measure $-s_2^{(2)}$ and (2) the wider literature demonstrating that excess entropy captures many of the effects that temperature, density, and confinement have on the transport coefficients of equilibrium fluids (see, e.g., Refs. 33–38). Although we focus exclusively on the quantity $-\tilde{s}_2$ in this paper to characterize dynamic structure, we have found that other commonly used structural order metrics⁴⁹ calculable from the τ -averaged $\tilde{g}_{2j}(r)$ produce qualitatively similar results.

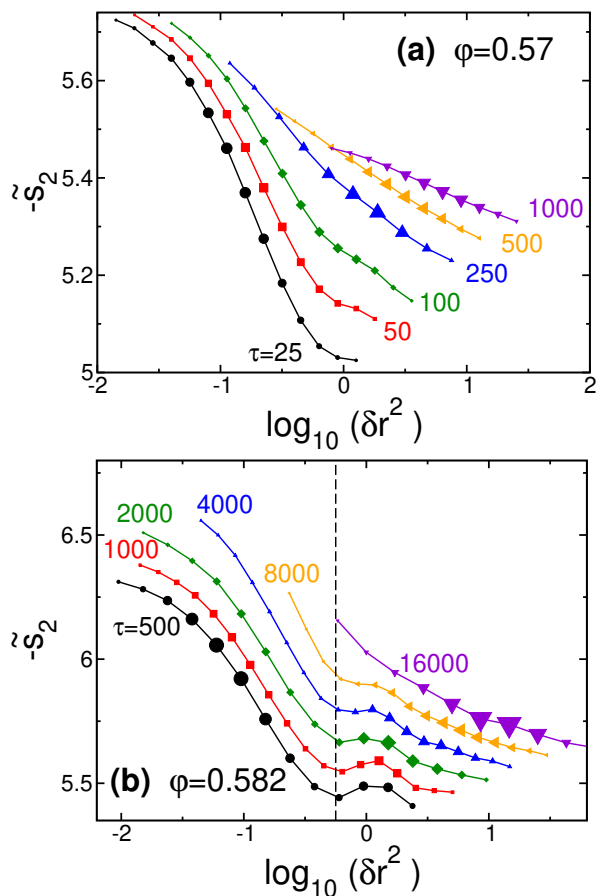


FIG. 3: (Color online) Metric for the average structural order, $-\tilde{s}_2$, that type 2 particles of the binary mixture discussed in the text experience during an observation time τ as a function of the logarithm of their mean-square displacement $\log_{10}(\delta r^2)$. Data is for packing fractions (a) $\varphi = 0.57$ and (b) $\varphi = 0.582$. The numbers in the figure correspond to the value of τ for the curve of the same color. The size of the symbol is proportional to the fraction of particles in the “mobility bin” centered at that value of $\log_{10}(\delta r^2)$. In (b), the horizontal dashed line at $\delta r^2 = 0.56$ represents the boundary between mobile and immobile particles (see Figure 2b and text).

To establish a baseline, we first examine the connection between displacement and average structural order (during displacement) for type 2 particles in the system at $\varphi = 0.57$, a supercooled fluid state point for which pronounced dynamic heterogeneities have not yet emerged. Figure 3a shows that, for all times spanning from the plateau region to the diffusive limit of the mean-square displacement curve in Figure 1, there is a clear negative correlation between the average structural order $-\tilde{s}_2$ surrounding a particle during an observation window τ and how far it moves in that time frame. As might be expected, the short-time curves are considerably steeper than longer-time curves. That is, for shorter time intervals, larger displacements are, on average, accompanied by progressively more local structural disordering (i.e., weakening of the pair correlations associated with the tagged particle). At longer times approaching the diffusive limit, particles sample a broader distribution containing larger mean-square displacements, and the correlation between average structure and dynamics of the tagged particle is reduced.

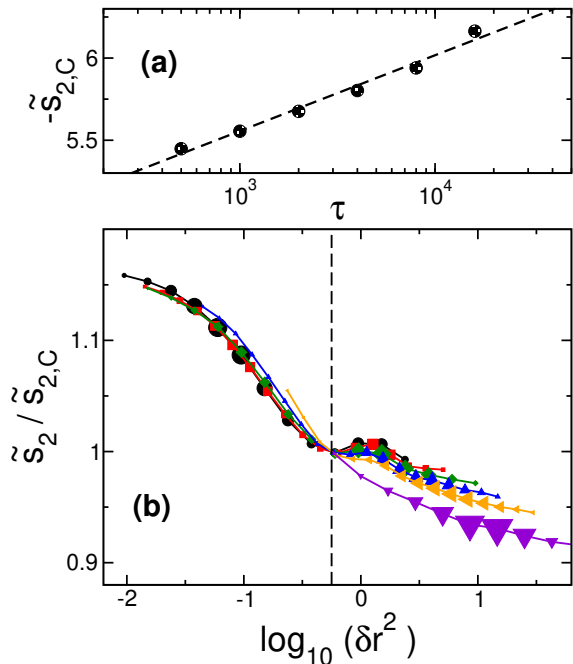


FIG. 4: (Color online) (a) The value of \tilde{s}_2 for $\delta r^2 = 0.56$, $\tilde{s}_{2,C} = \tilde{s}_2(\delta r^2 = 0.56)$, as a function τ . (b) Reduced measure of structural order $\tilde{s}_2/\tilde{s}_{2,C}(\tau)$ versus $\log_{10}(\delta r^2)$ for $\varphi = 0.582$. The data and symbols are the same as in Figure 3b.

The behavior is different, however, for the fluid at $\varphi = 0.582$ where the bifurcated displacement distribution characteristic of strong dynamic heterogeneities is observed (see Figure 3b). In particular, there is now a sharp change in the slope of the correlation between average structure and dynamics when one compares “immobile” versus “mobile” particles. For immobile caged particles, there is again a strong negative correlation between structural order and particle displacement; i.e., larger vi-

brational displacements are accompanied by increasingly weaker average pair correlations with neighboring particles. Moreover, the immobile particles sample a structural environment that is, on average, more ordered than mobile particles on the same time scale. However, *within the class of mobile particles* at a given time, the correlation between structural order and mobility is considerably weaker.

In fact, if we focus on the structure and dynamics of mobile particles, a minor secondary effect in Figure 3b is also apparent. Specifically, those particles with intermediate displacements (of the order of a single particle diameter) on a time scale τ can have slightly more average structural order than those with either smaller or larger displacements. This feature is likely due to recaging events,⁴³ where a new coordination shell is temporarily formed around a particle that has traveled just far enough to “break free” from its original set of nearest neighbors.

Another prominent feature of Figure 3b is that the curves for different τ have the same generic shape and appear merely shifted in terms of their average structural order. In fact, Fig 4(a) shows that the average structural order for particles with displacements at the boundary between immobile and mobile regions, i.e., $-\tilde{s}_{2,C} \equiv -\tilde{s}_2(\delta r^2 = 0.56)$, increases logarithmically with τ under these conditions. This result makes intuitive sense — more structural order is, on average, expected to surround particles that take a longer period of time to exhibit the same value of mean-square displacement. Interestingly, as we show in Fig 4(b), the τ dependence of Figure 3b is approximately removed altogether if one simply plots the average structural order of particles of a given mobility class normalized by its value at the boundary between mobile and immobile particles, $\tilde{s}_2/\tilde{s}_{2,C}$, versus $\log_{10}(\delta r^2)$. In other words, the overall “scale” of the structural order surrounding particles has a simple τ dependence for the intermediate times where dynamic heterogeneities are present ($500 \leq \tau \leq 8000$). The relative differences between the structures surrounding particles in different mobility classes, on the other hand, show only a very weak dependence on τ .

Although we do not yet have a theoretical model for predicting the average pair correlations of particles with different mobilities, the logarithmic time dependencies illustrated Fig. 4 are perhaps not too surprising when one considers the following. Mean-square displacements of a tagged particle over a time τ can be expressed $6D(\tau)\tau$. Little is known about how $D(\tau)$ relates to structure, but long-time self-diffusivities $D(\infty)$ exhibit an approximately exponential dependence on the two-body excess entropy^{34,47,48} for dense fluids. Thus, to first approximation, one might expect that particles which undergo the same mean-square displacement for different time scales τ share a constant value of the product $\tau \exp[\tilde{s}_2]$. Although this crude argument is consistent with the data of Fig. 4 and has some intuitive appeal, it is far from rigorous. More theoretical work will be needed to provide a

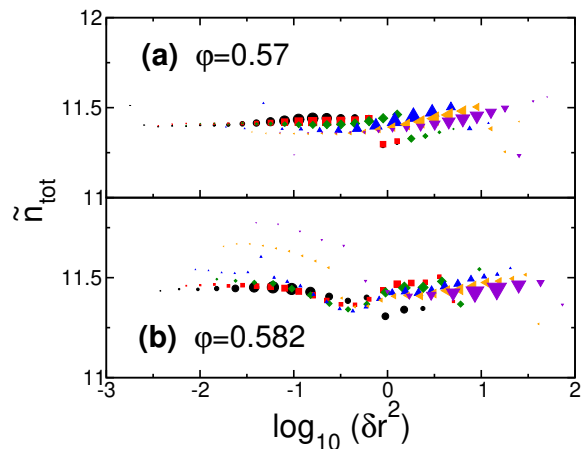


FIG. 5: (Color online) Average number of nearest neighbors, \tilde{n}_{tot} , for type 2 particles of the binary mixture discussed in the text during an observation time τ as a function of the logarithm of their mean-square displacement $\log_{10}(\delta r^2)$. Data is for packing fractions (a) $\varphi = 0.57$ and (b) $\varphi = 0.582$. The symbols are the same as those in Figure 3. The size of the symbols is proportional to the fraction of particles belonging to each mobility bin over time interval τ .

comprehensive understanding of the connections between dynamic structure and single-particle mobility observed here.

Given the above results, another question one might logically ask is whether a simpler measure like coordination number, which roughly characterizes local density surrounding a particle, might provide the same qualitative information as $-\tilde{s}_2$. To test this idea, we have also collected statistics on $\tilde{n}_{\text{tot}} \equiv 4\pi \sum_j x_j \rho \int_0^{r_{\text{min},j}} r^2 \tilde{g}_{2j}(r) dr$, the average number of nearest neighbors surrounding type 2 particles (in a given mobility bin on time interval τ). Here, $r_{\text{min},j}$ is the location of the first minimum in $\tilde{g}_{2j}(r)$. Figures 5a and b display \tilde{n}_{tot} as a function of $\log_{10}(\delta r^2)$ for $\varphi = 0.57$ and 0.582 , respectively. In contrast to $-\tilde{s}_2$, the average coordination number during the displacement does not provide a clear indication of the different structural environments that surround mobile versus immobile particles on intermediate time scales.

To summarize, we have presented computer simulation data on a model supercooled fluid showing a correlation between average structure and mean-square displacements that is qualitatively different for immobile and mobile particles over times relevant for dynamic heterogeneities. Interestingly, although the overall scale of the structural order depends logarithmically on observation time, the relative differences in structural order between mobile and immobile particles are largely independent of time. We provide a simple rationale for the aforementioned logarithmic time dependence, but more theoretical work is needed to fully understand these trends. Finally, we show that the aforementioned structural differences between particles with different mobilities are

not reflected by the coordination number.

In addition to further work on this problem in the arena of molecular simulation, it might be interesting to eventually explore whether the dynamical rules of kinetically constrained lattice models for supercooled liquids⁴⁰ produce behavior qualitatively consistent with that of Fig. 3 from our molecular dynamics simulations. It might also be interesting to compare these results to those from confocal microscopy experiments of dense colloidal suspensions.^{11,39}

We gratefully acknowledge helpful conversations with

Prof. K. S. Schweizer and P.L. Geissler about this work. Two authors (T.M.T. and V.G.) acknowledge support of the Welch Foundation (F-1696 and F-1599, respectively). One author (T.M.T) acknowledges financial support of the National Science Foundation (CTS-0448721) and the David and Lucile Packard Foundation. Another author (V.G.) acknowledges support from the US Army Research Office under Grant No. W911NF-07-1-0268. The Texas Advanced Computing Center (TACC) provided computational resources for this study.

-
- * Electronic address: truskett@che.utexas.edu; Corresponding Author
- ¹ D. N. Perera and P. Harrowell, Phys. Rev. E **54**, 1652 (1996).
 - ² W. Kob, C. Donati, S. J. Plimpton, P. H. Poole, and S. C. Glotzer, Phys. Rev. Lett. **79**, 2827 (1997).
 - ³ C. Donati, J. F. Douglas, W. Kob, S. J. Plimpton, P. H. Poole, and S. C. Glotzer, Phys. Rev. Lett. **80**, 2338 (1998).
 - ⁴ R. Yamamoto and A. Onuki, Phys. Rev. E **58**, 3515 (1998).
 - ⁵ C. A. Angell, K. L. Ngai, G. B. McKenna, P. F. McMillan, and S. W. Martin, J. Appl. Phys. **88**, 3113 (2000).
 - ⁶ M. D. Ediger, Annu. Rev. Phys. Chem. **51**, 99 (2000).
 - ⁷ K. S. Schweizer, Curr. Opin. Colloid In. **12**, 297 (2007).
 - ⁸ E. Vidal Russell and N. E. Israeloff, Nature **408**, 695 (2000).
 - ⁹ S. C. Glotzer, V. N. Novikov, and T. B. Schröder, J. Chem. Phys. **112**, 509 (2000).
 - ¹⁰ S. C. Glotzer, J. Non-Cryst. Solids **274**, 342 (2000).
 - ¹¹ E. R. Weeks, J. C. Crocker, A. C. Levitt, A. Schofield, and D. A. Weitz, Science **287**, 627 (2000).
 - ¹² Y. Gebremichael, T. B. Schröder, F. W. Starr, and S. C. Glotzer, Phys. Rev. E **64**, 051503 (2001).
 - ¹³ N. Lačević, F. W. Starr, T. B. Schröder, and S. C. Glotzer, J. Chem. Phys. **119**, 7372 (2003).
 - ¹⁴ M. Vogel and S. C. Glotzer, Phys. Rev. Lett. **92**, 255901 (2004).
 - ¹⁵ T. Kawasaki, T. Araki, and H. Tanaka, Phys. Rev. Lett. **99**, 215701 (2007).
 - ¹⁶ H. C. Andersen, Proceedings of the National Academy of Sciences of the United States of America **102**, 6686 (2005).
 - ¹⁷ R. Richert, J. Phys.: Condens. Matter **14**, R703 (2002).
 - ¹⁸ R. Yamamoto and A. Onuki, Phys. Rev. Lett. **81**, 4915 (1998).
 - ¹⁹ A. M. Puertas, M. Fuchs, and M. E. Cates, cond-mat **1**, 0510443 (2005).
 - ²⁰ D. R. Reichman, E. Rabani, and P. L. Geissler, J. Phys. Chem. B **109**, 14654 (2005).
 - ²¹ E. J. Saltzman and K. S. Schweizer, Phys. Rev. E **74**, 061501 (2006).
 - ²² E. J. Saltzman and K. S. Schweizer, Phys. Rev. E **77**, 051504 (2008).
 - ²³ F. H. Stillinger and J. A. Hodgdon, Phys. Rev. E **50**, 2064 (1994).
 - ²⁴ G. Tarjus and D. Kivelson, J. Chem. Phys. **103**, 3071 (1995).
 - ²⁵ S. K. Kumar, G. Szamel, and J. F. Douglas, J. Chem. Phys. **124**, 214501 (2006).
 - ²⁶ B. Doliwa and A. Heuer, J. Phys.: Condens. Matter **11**, A277 (1999).
 - ²⁷ A. Widmer-Cooper, P. Harrowell, and H. Fynewever, Phys. Rev. Lett. **93**, 135701 (2004).
 - ²⁸ L. Berthier and R. L. Jack, Phys. Rev. E **76**, 041509 (2007).
 - ²⁹ A. Widmer-Cooper and P. Harrowell, J. Phys.: Condens. Matter **17**, S4025 (2005).
 - ³⁰ A. Widmer-Cooper and P. Harrowell, Phys. Rev. Lett. **96**, 185701 (2006).
 - ³¹ A. Widmer-Cooper and P. Harrowell, J. Non-Cryst. Solids **352**, 5098 (2006).
 - ³² A. Widmer-Cooper and P. Harrowell, J. Chem. Phys. **126**, 154503 (2007).
 - ³³ Y. Rosenfeld, J. Phys.: Condens. Matter **11**, 5415 (1999).
 - ³⁴ M. Dzugasov, Nature **381**, 137 (1996).
 - ³⁵ J. Mittal, J. R. Errington, and T. M. Truskett, Phys. Rev. Lett. **96**, 177804 (2006).
 - ³⁶ G. Goel, W. P. Krekelberg, M. J. Pond, J. Mittal, V. K. Shen, J. R. Errington, and T. M. Truskett, J. Stat. Mech. **2009**, P04006 (2009).
 - ³⁷ W. P. Krekelberg, M. J. Pond, G. Goel, V. K. Shen, J. R. Errington, and T. M. Truskett, Phys. Rev. E **80**, 061205 (2009).
 - ³⁸ N. Gnan, T. B. Schroder, U. R. Pedersen, N. P. Bailey, and J. P. Dyre, J. Chem. Phys. **131**, 234504 (2009).
 - ³⁹ W. K. Kegels and A. van Blaaderen, Science **287**, 290 (2000).
 - ⁴⁰ F. Ritort and P. Sollich, Adv. Phys. **52**, 219 (2003).
 - ⁴¹ D. C. Rapaport, *The Art of Molecular Dynamic Simulation* (Cambridge University Press, Cambridge, 2004), 2nd ed.
 - ⁴² C. R. Nugent, K. V. Edmond, H. N. Patel, and E. R. Weeks, Phys. Rev. Lett. **99**, 025702 (2007).
 - ⁴³ E. R. Weeks and D. A. Weitz, Phys. Rev. Lett. **89**, 095704 (2002).
 - ⁴⁴ M. E. Cates, M. Fuchs, K. Kroy, W. C. K. Poon, and A. M. Puertas, J. Phys.: Condens. Matter **16**, S4861 (2004).
 - ⁴⁵ C. Donati, S. C. Glotzer, P. H. Poole, W. Kob, and S. J. Plimpton, Phys. Rev. E **60**, 3107 (1999).
 - ⁴⁶ R. Palomar and G. Sesé, J. Chem. Phys. **129**, 064505 (2008).
 - ⁴⁷ A. Samanta, S. M. Ali, and S. K. Ghosh, Phys. Rev. Lett. **87**, 245901 (2001).
 - ⁴⁸ M. J. Pond, W. P. Krekelberg, V. K. Shen, J. R. Errington, and T. M. Truskett, J. Chem. Phys. **131**, 161101 (2009).
 - ⁴⁹ T. M. Truskett, S. Torquato, and P. G. Debenedetti, Phys. Rev. E **62**, 993 (2000).